ELSEVIER

Infrared Physics & Technology 43 (2002) 245–250

INFRARED PHYSICS & TECHNOLOGY

www.elsevier.com/locate/infrared

Dual ion beam sputtering vanadium dioxide microbolometers by surface micromachining

D. Zintu *, G. Tosone, A. Mercuri

Consorzio CREO, via Pile 60, 67100 l'Aquila, Italy

Abstract

Suspended microbolometers have been realized by surface micromachining. The sensible film was vanadium dioxide, deposited by the dual ion beam sputtering technique. The film has a TCR of $-3\%\,K^{-1}$ and a resistivity of few Ω cm. The best performances measured on such microbolometers are close to the state of the art: the detectivity is up to 10^8 cm $Hz^{1/2}$/W and the response time is few milliseconds. © 2002 Elsevier Science B.V. All rights reserved.

1. Introduction

In the last years microbolometers are becoming very interesting for IR imaging and detection.

In the past, this field was mainly of military interest and photon detectors have been used. Today a lot of civil employments of IR detection have been pointed out [1,2] and the market is asking for devices at lower cost. IR photon detectors have better performances [3] (a detectivity in the range of 10^{10} cm $Hz^{1/2}$/W and a response time of microseconds), but they are very expensive, because, for having such performances, they must be cooled at cryogenic temperature. On the contrary microbolometers [4] are cheap and can reach quite good performances (a detectivity in the range of 10^8 cm $Hz^{1/2}$/W and a response time of milliseconds), enough for civil applications. The possibility to work at room temperature and the full integrability on silicon are two of the main reasons of the low cost of microbolometers.

Microbolometers are thermal detectors [5]: the radiation is absorbed by a sensible material, that turns temperature changes into measurable resistance changes. To have the highest sensibility, the thermal conductance between the sensible film and the substrate must be minimized: for this reason the sensible film of microbolometers is deposited on a suspended thermally insulating membrane. To have also a fast response time, also the thermal capacity must be minimized.

Bulk and surface micromachining [6] are the commonly used technologies to realize suspended membranes on silicon. The second one is more useful for detectors of small area and for arrays in which the maximum fill factor is desired. Honeywell Technology Center [7,8] and the Defence Science and Technology Organisation [9] were two of the first centers of research to realize arrays of microbolometers using surface micromachining. Today the best results reached in the field are microbolometers arrays of 320×240 devices with an active area of 50×50 μm^2, having a detectivity

* Corresponding author. Tel.: +39-862-346-207; fax: +39-862-346-201.

E-mail address: dzintu@tin.it (D. Zintu).

1350-4495/02/$ - see front matter
PII: S1350-4495(02)00147-0

$\approx 5 \times 10^8$ cm $Hz^{1/2}$/W and a response time of few milliseconds [10].

The mainly used sensible materials in microbolometers are: hydrogenated silicon, germanium and silicon–germanium alloys, in amorphous or polycrystalline forms (with a TCR up to $-5.0\%\,K^{-1}$) [9,11], the superconductor YBCO [12] and amorphous vanadium oxides (with a TCR up to $-2.5\%\,K^{-1}$) [10,13]. Chemical vapour deposition (CVD) and sputtering are the techniques used to deposit such sensible materials.

At CREO we have realized microbolometers by surface micromachining, using as a sensible material vanadium dioxide deposited for the first time by the dual ion beam sputtering (DIBS) technique. The higher absolute value of TCR obtained is $-5.5\%\,K^{-1}$.

Using this material, we have obtained the best performances with microbolometers of active area $\approx 100 \times 100$ μm^2, showing a responsivity $> 10^3$ V/W, a response time of few milliseconds, a noise in the range of 10^{-7} V/$Hz^{-1/2}$ and a detectivity up to 10^8 cm $Hz^{1/2}$/W. Devices optimization is in progress.

2. Experimental

To deposit the sensible material films we used the DIBS technique.

Depositing by ion beams has a lot of advantages in comparison with the simple sputtering [14]. In fact it is possible to tune independently each deposition parameter: deposition pressure, ion current and energy. Moreover there is no plasma contamination on the films because the plasma generation zone and the substrate zone are far apart.

CREO's DIBS is equipped with two Ion Tech RF ion sources (Fig. 1): the first impinges on the target and the second directly against the substrate, to make assisted depositions. The chamber is evacuated by a Leybold cryopump with a residual pressure in the low 10^{-7} Torr and the depositions were made maintaining a pressure of about $1–2 \times 10^{-4}$ Torr. The deposition gun is at 45° oriented with respect to the target and the target is at 45° with respect to the substrate.

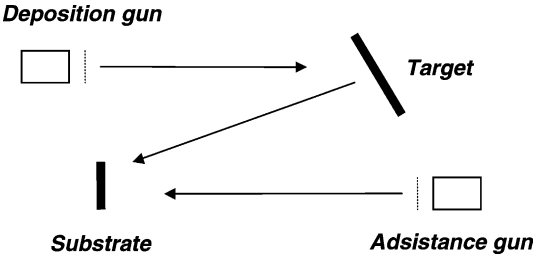

Fig. 1. DIBS scheme.

To improve films uniformity the substrate spins around its normal axis. In both the ion guns is possible to use neutral or reactive gases.

The film of mechanical support (Si_3N_4) and the electric contacts (NiCr/Au) were deposited by sputtering, using RF magnetron and DC alimentations respectively. CREO's sputtering is equipped with a turbomolecular pump and the residual pressure is in the high 10^{-7} Torr.

TCR was measured in a thermal bath by a Kitley multimeter, exploring a thermal range of 10–50 °C. Morphological informations were obtained from SEM images.

Devices full electrical characterization was made by CREO's complete setup: IV Keathley 236, multimeter HP 3458A with highest resistance detectable 1.2 GΩ, cryostat Cryophysics with ZnSe window that can be evacuated until 10^{-5} Torr by rotative-turbomolecular pumps, thermal stabilizator Lakeshore 220 with PID temperature controller, FFT analyzer SR780 Stanford, black body CI SR20 with temperature range 70–1000 °C and resolution 1 °C.

Thermal parameters were measured indirectly.

3. Results

Depositing by DIBS, different vanadium oxides stoichiometry have been explored, with a resistivity in the range of 10^{-3}–10^3 Ω cm and relative values of TCR between -0.1 and $-5.5\%\,K^{-1}$. Fig. 2 shows that increasing resistivities are related with increasing absolute values of TCR.

To realize the samples, all the DIBS chances have been stressed, starting always from the same vanadium pentoxide target:

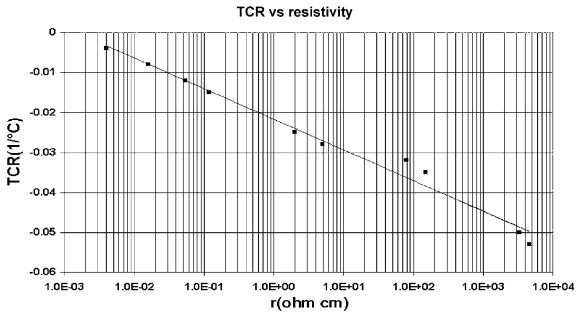

Fig. 2. VO_2 TCR versus resistivity.

(a) we deposited using only the deposition gun, fed by argon, changing the substrate temperature,
(b) we deposited like in (a), introducing also non-ionized oxygen into the chamber and changing the ratio of the partial pressures between argon and oxygen,
(c) we deposited like in (a), using also the assistance gun, fed by argon, and changing beam energy and current,
(d) we deposited like in (a), using also the assistance gun fed by oxygen, changing beam energy and current, and varying the ratio of the partial pressure between argon and oxygen.

The higher TCR in absolute value has been measured in films of stoichiometry close to vanadium pentoxide. Unfortunately, the relative resistivity is in the order of $10^3\ \Omega$cm, too high for having the desired value of sheet resistance (about 100 k$\Omega/\square$) with a film few thousands of angstroms thick. Moreover vanadium pentoxide has been found soluble in water, therefore incompatible with all the photolithography pattern transfer processes.

For this reason, the best sensible film for realizing microbolometers with our process is a film with a stoichiometry close to vanadium dioxide. It has a TCR of $-3.0\%\,K^{-1}$ and a resistivity of about 1 Ωcm. A film of such a material has the desired sheet resistance if its thickness is about 2000 Å, suitable to minimize the thermal capacity of the devices. Moreover this oxide and its properties are stable with the time and it is neither soluble in water nor in any solvent used in the realization process.

The vanadium dioxide we deposit is amorphous, and its electrical conduction [15] is due to thermally activated electron hopping between impurities sites. The resistance has an Arrhenius behaviour respect to the temperature, like $R \propto \exp(E_{act}/kT)$, where E_{act} is the activation energy for the conduction, related to the TCR by the equation $\mathrm{TCR} = -E_{act}/kT^2$. A plot of the resistance slope versus the temperature is shown in Fig. 3 and the relative TCR in Fig. 4.

Using this material for realizing microbolometers, we obtained the performances that will follow.

Fig. 5 shows microbolometers realization steps by surface micromachining. At first a sacrificial layer of polyimide is spinned and patterned on the ordinarily cleaned silicon substrate. Then the

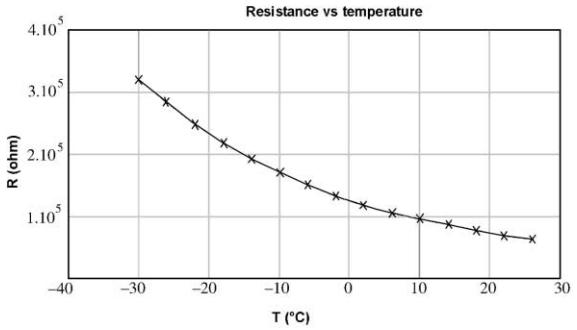

Fig. 3. VO_2 sheet resistance versus temperature.

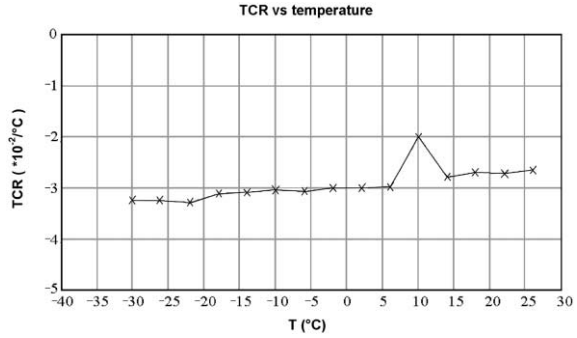

Fig. 4. VO_2 TCR versus temperature.

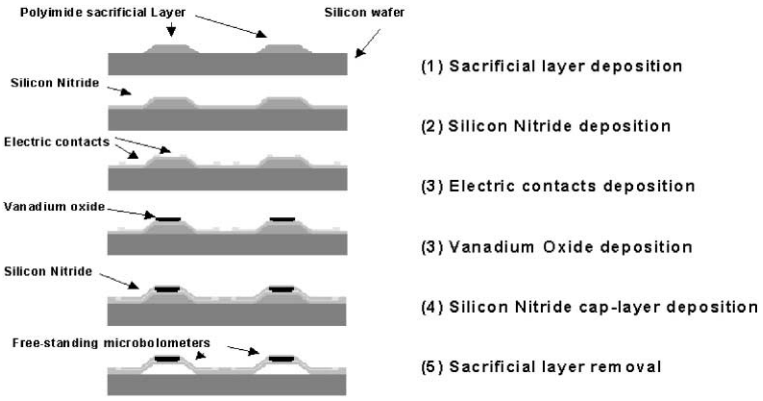

Fig. 5. Fabrication steps of microbolometers using surface micromachining.

mechanical support film (silicon nitride), the electric contacts (NiCr/Au), the sensitive material, and a silicon nitride cap layer are deposited. At the end the polyimide is removed and the device remains suspended with respect to the silicon substrate.

The best result has been obtained on devices having an active area of 100×100 μm^2. A SEM image of one of these devices is shown in Fig. 6: the bridge structure is well visible. The responsivity, measured at 20 Hz versus bias current, is shown in Fig. 7: it has a maximum at ≈25 μA where it is equal to 3.5 kV/W and then decreases to 1 kV/W at ≈100 μA. Scanning the chopper frequency and biasing the devices at 30 μA, the responsivity versus frequency plot has been obtained (Fig. 8): the slope decreases like the well-known equation [5] $\mathrm{Resp}(\omega) \propto \mathrm{Resp}_{\mathrm{DC}}(1/\sqrt{1+\omega^2\tau^2})$. Calculating τ from the plot it results as $\tau \approx 5$ ms.

The measured thermal conductance is $\approx 10^{-5}$ W/K and the thermal capacity is $\approx 5 \times 10^{-8}$ J/K.

The noise has a $1/f$ behaviour: biasing the device by 45 μA current, noise ranges between 1×10^{-6} V/Hz$^{1/2}$ at 10 Hz and 3×10^{-7} V/Hz$^{1/2}$ at 100 Hz, as shown in Fig. 9. The simulated continuous line has been calculated from a $1/f$ noise model [16] and the dashed one from a Johnson noise one [17].

The detectivity versus bias current is shown in Fig. 10: it is in the range of 10^8 cm Hz$^{1/2}$/W for bias current >50 μA.

The performances of our devices are close to the state of the art in the field, with the sensible material deposited by the new DIBS technique. In

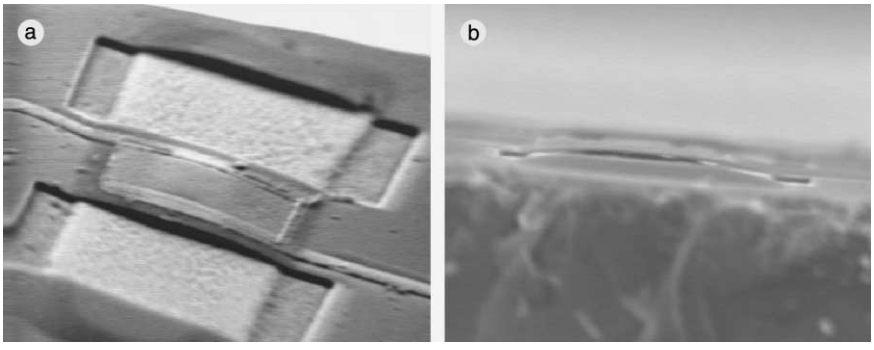

Fig. 6. SEM images of a microbolometer of active area ≈100×100 μm^2: (a) *xy* view and (b) *xz* view.

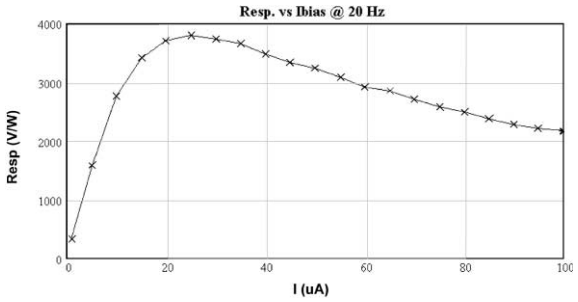

Fig. 7. Microbolometers responsivity versus bias current.

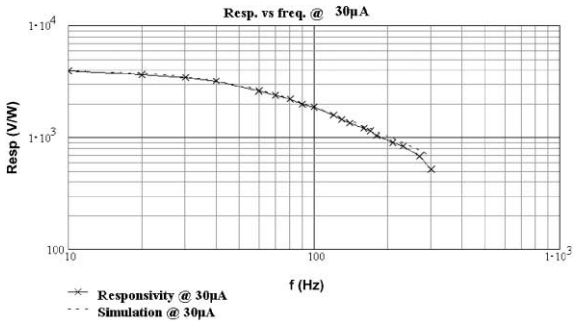

Fig. 8. Microbolometers responsivity versus frequency.

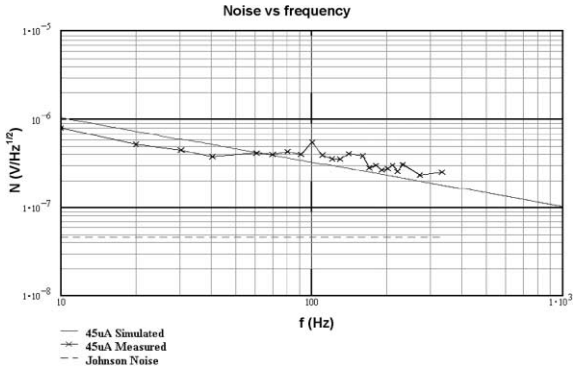

Fig. 9. Microbolometers noise at 45 μA bias current versus frequency.

particular, comparing our work with others, it must be underlined that our microbolometers have not an absorber structure, and this fact is estimated [5] to decrease normally the responsivity of

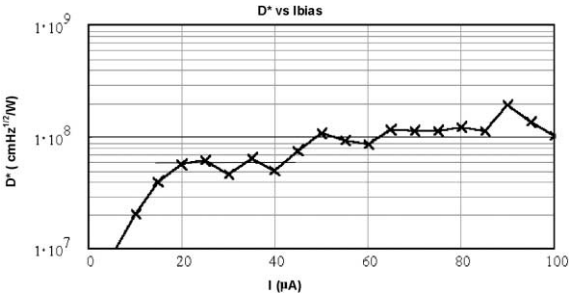

Fig. 10. Microbolometers detectivity versus bias current.

an order of magnitude. We are going to fabricate microbolometers with an integrated absorber.

4. Conclusions

Microbolometers prototypes have been realized using amorphous VO_2, deposited by DIBS, as sensible material. The TCR is $\approx -3.0\%\,K^{-1}$. Devices performances are close to the state of the art: a detectivity up to 10^8 cm $Hz^{1/2}/W$ and a response time of few milliseconds have been measured. Devices optimization is in progress.

References

[1] A. Rogalski, in: Proceedings of the 4th International Workshop on Advanced Infrared technology and Application, CNR-IROE; Firenze, September 15–16, 1997.
[2] C. Corsi, in: Proceeding of the 5th AITA, Venezia, September 29–30, 1999, pp. 3–9.
[3] E.L. Dereniak, G.D. Boreman, Infrared Detectors and Systems, John Wiley & Sons, New York, 1996 (Chapters 7 and 8).
[4] E.L. Dereniak, G.D. Boreman, Infrared Detectors and Systems, John Wiley & Sons, New York, 1996, pp. 408–423 (Chapter 9).
[5] R.A. Wood, Uncooled infrared imaging arrays and systems, Semiconductors and Semimetals, vol. 47, Academic Press, San Diego, 1997, pp. 45–98 (Chapter 3).
[6] R.A. Wood, Uncooled infrared imaging arrays and systems, Semiconductors and Semimetals, vol. 47, Academic Press, San Diego, 1997, pp. 98–109 (Chapter 3).
[7] R.A. Wood, B.E. Cole, C.J. Han, R. Higashi, D. Nielsen, A. Weinstein, in: Proceedings of the GOMAC, Orlando, November 1991.
[8] R.A. Wood, C.J. Han, P.W. Kruse, in: Proceedings of the IEEE Solid State Sensors and Actuators Workshop, Hilton Head Island, SC, June 1992, pp. 132–135.

[9] M.H. Unewisse, B.I. Craig, R.J. Watson, O. Reinhold, K.C. Liddiard, Proc. SPIE 2554 (1995) 43–54.
[10] H. Jerominek, T.D. Pope, M. Renaud, N.R. Swart, F. Picerd, M. Lehoux, S. Savard, G. Bilodeau, D. Audet, Proc. SPIE 3061 (1997) 236–247.
[11] J. Tissot, F. Rothan, C. Vedel, M. Vilain, J. Yon, LETI/LIR's Amorphous Silicon Uncooled Microbolometers Development, Orlando, 1998.
[12] R. Barth, J. Siewert, C. Jaekel, B. Spengenberg, H. Kurz, W. Prusseit, B. Utz, H. Wolf, J. Appl. Phys. 78 (1995) 4218–4221.
[13] R.A. Wood, Proc. SPIE (July) (1993).
[14] J.J. Cuomo, S.M. Rossnagel, H.R. Kaufman, Handbook of Ion Beam Processing Technology, Noyes publications, Park Ridge, New Jersey, USA, 1989.
[15] I.G. Austin, N.F. Mott, Science 168 (1970) 3927.
[16] K.R. Laker, W.M.C. Sansen, Design of Analog Integrated Circuits and Systems, McGraw-Hill, Singapore, p. 75 (Chapter 1).
[17] E.L. Dereniak, G.D. Boreman, Infrared Detectors and Systems, John Wiley & Sons, New York, 1996, pp. 168–173 (Chapter 5).